

Charge-disproportionation-induced magnetic glassy behavior in $\text{La}_{0.5}\text{Ca}_{0.5}\text{FeO}_{3-\delta}$

Ya-Qiong Liang, Nai-li Di, and Zhao-hua Cheng*

State Key Laboratory of Magnetism, Institute of Physics, Chinese Academy of Sciences, Beijing 100080, China

(Received 9 May 2005; revised manuscript received 11 August 2005; published 14 October 2005)

The magnetic properties of $\text{La}_{0.5}\text{Ca}_{0.5}\text{FeO}_{3-\delta}$ perovskites with different oxygen vacancy contents were comprehensively investigated by means of x-ray diffraction, Mössbauer spectroscopy, and magnetization measurements. A glassy magnetic behavior was observed by the dc magnetization and ac susceptibility measurements. Around the freezing temperature, a charge disproportionation (CD) phase transition from Fe^{4+} ions to Fe^{3+} and Fe^{5+} ions was detected by ^{57}Fe Mössbauer spectra. Due to the competition between Fe^{3+} — Fe^{5+} ferromagnetic interaction and Fe^{3+} — Fe^{3+} antiferromagnetic interaction, the CD transition from Fe^{4+} ions to Fe^{3+} and Fe^{5+} ions induces the glassy magnetic behavior.

DOI: 10.1103/PhysRevB.72.134416

PACS number(s): 75.10.Nr, 82.30.Hk, 76.80.+y, 75.40.Gb

I. INTRODUCTION

In recent years, much attention has been paid on the electronic states and unusual physical properties of transition-metal oxides with strong electron correlation. In highly covalent transition-metal perovskite-type oxides containing $d^4(\text{Fe}^{4+}, \text{Mn}^{3+})$ or $d^7(\text{Ni}^{3+})$ ions, such as $\text{La}_{1-x}\text{Sr}_x\text{FeO}_3$, NdNiO_3 , etc., a charge disproportionation (CD) transition was often observed, in which a charge state is separated into two different charge states as $2d^n \rightarrow d^{n-1} + d^{n+1}$.^{1,2} The CD transition exists the alternating-valence group containing ions in two valence states differing by $2e$ (on-site pairs) and sometimes exhibiting charge ordering (CO) and orbital ordering.³ For example, CaFeO_3 shows the CD and CO transition at 290 K accompanied with a structural transition from $Pbnm$ in the normal state to $P2/n$ in the CO state and a magnetic phase transition from antiferromagnetic (AFM) metallic state to CO insulating state.⁴ CO sequence of $\text{Fe}^{5+}\text{Fe}^{3+}\text{Fe}^{3+}\text{Fe}^{5+}\text{Fe}^{3+}\text{Fe}^{3+}\dots$ along the body diagonal [111] direction of $\text{La}_{1/3}\text{Sr}_{2/3}\text{FeO}_3$ single crystal was resulted from the CD transition of Fe^{4+} ions.^{5,6} The mechanism of CD transition, which is related to the order-disorder of charge, spin and orbital, is a very important issue in transition-metal oxides with strong electron correlation in light of the magnetic phase transition and electronic states.

^{57}Fe Mössbauer spectroscopy provides a powerful technique for probing the charge states of Fe ions since different Fe charge states possess different magnetic hyperfine fields and isomer shifts. The CD transition can be investigated by ^{57}Fe Mössbauer spectra measured at various temperatures. In previous work, Mössbauer spectra indicated that the Fe^{4+} ions in $\text{La}_{1-x}\text{Ca}_x\text{FeO}_{3-\delta}$ are not stable in low temperature region and tends to come through CD,^{7,8} but the correlation of CD with the magnetic phase transition is not yet well understand. It was known that the superexchange interaction between Fe^{3+} ($3d^5$) and Fe^{5+} ($3d^3$) along the 180° Fe—O—Fe pathway is ferromagnetic (FM), whereas the superexchange interaction between Fe^{3+} and Fe^{3+} or Fe^{5+} and Fe^{5+} is antiferromagnetic,^{9,10} the competition between FM exchange interactions and AFM ones may result in a micro-magnetism or cluster-glass-like magnetic behavior. In this work, $\text{La}_{0.5}\text{Ca}_{0.5}\text{FeO}_{3-\delta}$ perovskites prepared under air and

oxygen atmosphere were selected to investigate the effect of CD on magnetic properties by means of magnetization measurements and ^{57}Fe Mössbauer spectroscopy.

II. EXPERIMENTAL DETAILS

The traditional solid-state reaction method was employed to prepare $\text{La}_{0.5}\text{Ca}_{0.5}\text{FeO}_{3-\delta}$ polycrystalline powders. Accurately weighed amounts of pure La_2O_3 , CaCO_3 , and Fe_2O_3 (99.9%) powders with stoichiometric ratios appropriate for $\text{La}_{0.5}\text{Ca}_{0.5}\text{FeO}_3$ were mixed in an agate mortar. The powders were subsequently preheated between 900°C and 1000°C with intermediate grindings. In order to investigate the effect of oxygen vacancies on the magnetic properties, the products were divided into two portions, pressed into pellets and fired at 1300°C in air, sample A (SA), and flowing 100% oxygen of 1 atm, sample O (SO), respectively; followed by slow cooling to room temperature.

Phase analysis and lattice parameters were determined by x-ray diffraction (XRD) with $\text{Cu } K\alpha$ radiation. The magnetization measurements were performed by a commercial superconducting quantum interference device (SQUID) magnetometer. ac susceptibility measurements were performed on a commercial physical properties measurements system (Quantum Design, PPMS-14). ^{57}Fe Mössbauer spectra from 20 K to room temperature were recorded by a Wissel system constant acceleration Mössbauer spectrometer with a ^{57}Co (Rh) source. A CCS-850 optical exchange helium gas closed cycle refrigerator was employed to provide variable temperatures from 20 K to room temperature. The velocity was calibrated using an α -Fe foil. The values of center shifts given here are relative to α -Fe at room temperature.

III. RESULTS AND DISCUSSIONS

Figure 1 illustrates the observed and fitted XRD patterns of $\text{La}_{0.50}\text{Ca}_{0.50}\text{FeO}_{3-\delta}$ perovskites prepared in air (SA) and oxygen atmospheres (SO). XRD patterns reveal that these two samples are single phase with an orthorhombically distorted perovskite structure ($Pbnm$ space group). Rietveld profile refinement was carried out to determine lattice constants and atomic positions. In the orthorhombic structure,

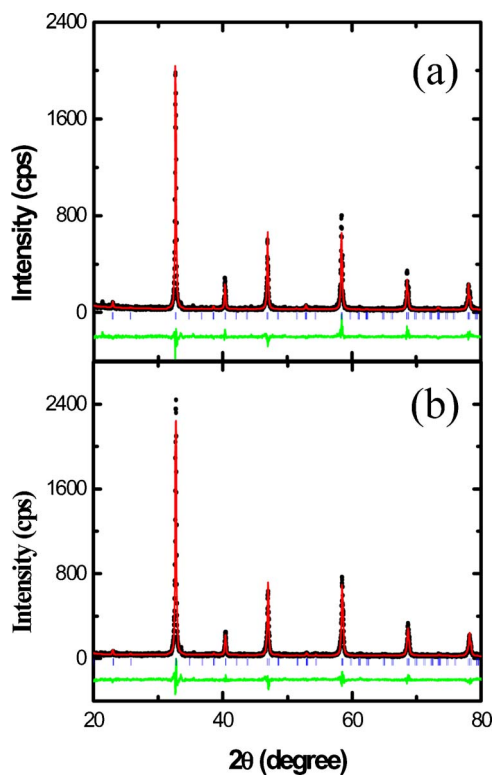


FIG. 1. (Color online) Observed and fitted XRD patterns of $\text{La}_{0.50}\text{Ca}_{0.50}\text{FeO}_{3-\delta}$ perovskites prepared in air (a) and oxygen atmospheres (b).

oxygen ions occupy two nonequivalent sites, namely $\text{O}_I(4c)$ and $\text{O}_{II}(8d)$, with a population ratio of 1:2. Six O^{2-} ions (two O_I and four O_{II}) surround each Fe ion and form an octahedron. Refined values of the lattice and positional parameters and atomic occupancies at room temperature are summarized in Table I. The lattice constants are found to be in excellent agreement with the earlier results.^{7,8} Within the experimental error, the average Fe—O bond length in SO and SA is almost invariable, whereas the Fe— O_{II} —Fe bond angle in SO is much closer to 180° than that in SA.

Figure 2 illustrates the M-H curves of SA and SO cooled from 300 K to 5 K without external magnetic field. The

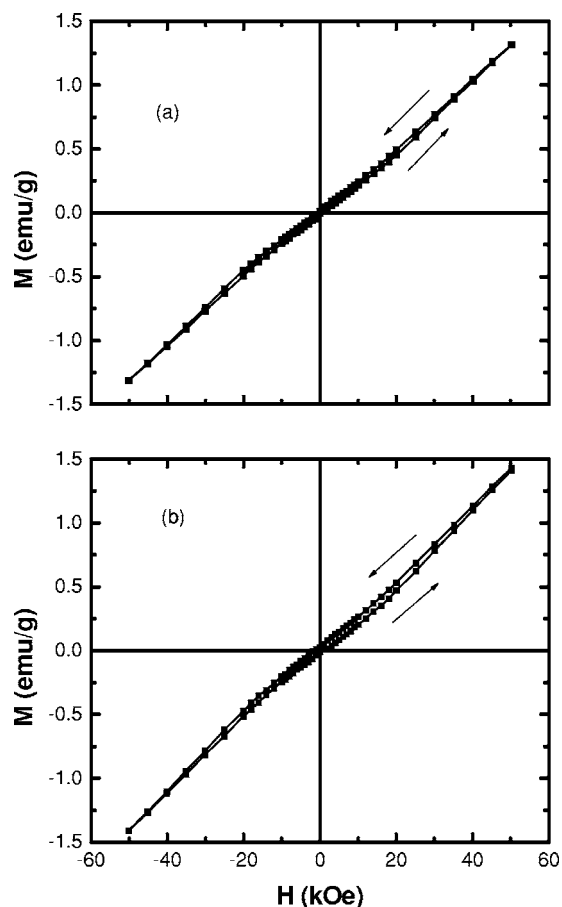


FIG. 2. Zero-field-cooled hysteresis loops measured at 5 K for SA (a) and SO (b).

magnetization at 5 K varies almost linearly with the external magnetic field and does not saturate even up to 50 kOe. This confirms the antiferromagnetic order at low temperatures. However, a slight deviation from straight line and irreversibility in magnetization between field-increasing procedure and field-decreasing one implies that these two samples exhibit a spin-canted magnetism or cluster-glass-like behavior.

To distinguish the spin-canted magnetism and clusterlike magnetic behavior of these two samples, temperature depen-

TABLE I. Refinement parameters of $\text{La}_{0.5}\text{Ca}_{0.5}\text{FeO}_{3-\delta}$ at room temperature.

Lattice constants	Lattice coordinate	Lattice coordinate		Fe—O		Fe—O—Fe		Reliability factor	
		x	y	z	Fe— O_I	Fe— O_{II}	Fe— O_I —Fe		Fe— O_{II} —Fe
SA $a=5.461(2)$ Å $b=5.461(1)$ Å $c=7.737(1)$ Å	La/Ca(4c)	0.498(3)	-0.005(1)	0.250(0)	2.062(1)	1.954(3)	139.3(6)	171.4(3)	$R_{wp}=11.047$ $R_p=14.028$ $\chi^2=1.003$
	Fe(4a)	0.000(0)	0.000(0)	0.000(0)		1.919(2)			
	$\text{O}_I(4c)$	0.123(1)	0.030(9)	0.250(0)					
	$\text{O}_{II}(8d)$	0.271(6)	0.234(4)	0.004(4)					
SO $a=5.458(1)$ Å $b=5.459(1)$ Å $c=7.740(1)$ Å	La/Ca(4c)	0.499(3)	0.014(1)	0.250(0)	2.055(1)	2.007(1)	139.0(5)	174.5(2)	$R_{wp}=10.824$ $R_p=13.570$ $\chi^2=1.024$
	Fe(4a)	0.000(0)	0.000(0)	0.000(0)		1.868(1)			
	$\text{O}_I(4c)$	0.131(1)	-0.021(4)	0.250(0)					
	$\text{O}_{II}(8d)$	0.235(6)	0.252(4)	0.002(4)					

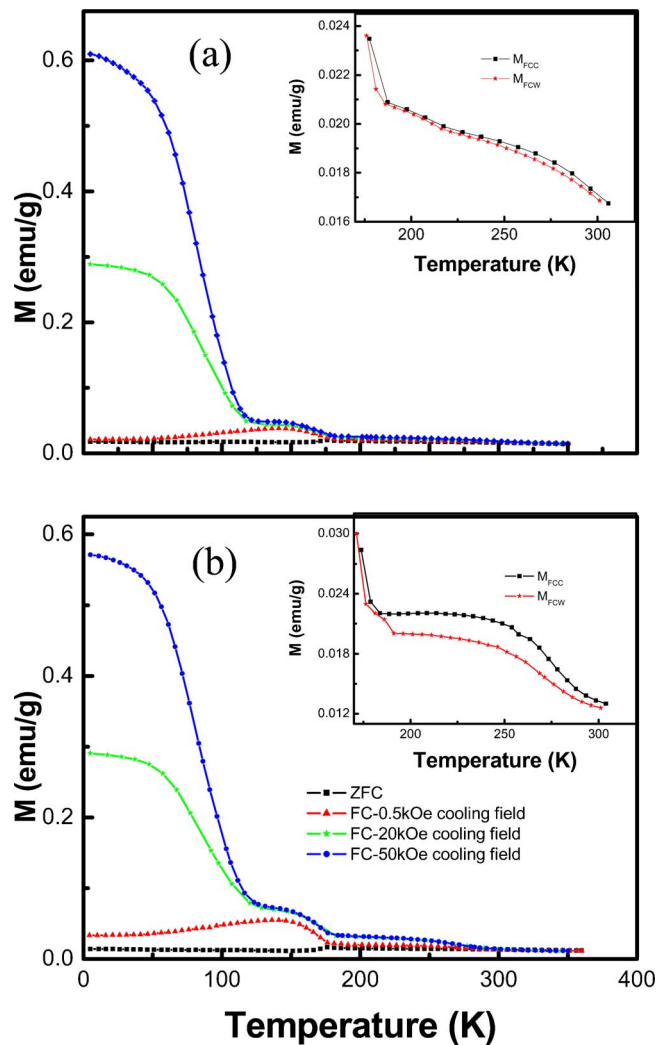


FIG. 3. (Color online) Temperature dependence of magnetization at different cooling field under 500 Oe applied field ($H_{FC}=0, 0.5, 30,$ and 50 kOe). The inset shows the temperature dependence of magnetization under the process of FCC and FCW. (a) SA, (b) SO.

dence of zero-field-cooled (ZFC) and field-cooled (FC) dc magnetization for SA and SO was measured in the applied field of 500 Oe and illustrated in the main plot of Figs. 3(a) and 3(b), respectively. Since no difference in magnetization between ZFC and FC processes in the “spin-canted” system, the divergence between M_{ZFC} and M_{FC} around 175 K suggests that there exists a magnetic glassy behavior.¹¹ In contrast to other spin-glass systems, in which a small cooling-field induces a large increase in the magnetization, a significant increase in magnetization for FC curves is achieved when the cooling field is higher than 30 kOe. This result suggests that the antiferromagnetic coupling in these Fe-based perovskites is much stronger than the ferromagnetic coupling.

Above the freezing temperature $T_f=175$ K, it seems that a ferromagnetic-like thermomagnetization curve was observed in the temperature range of ~ 175 – 280 K, as shown in the insets of Fig. 3. In order to check whether ferromagnetic component exists in the temperature region, the magnetization

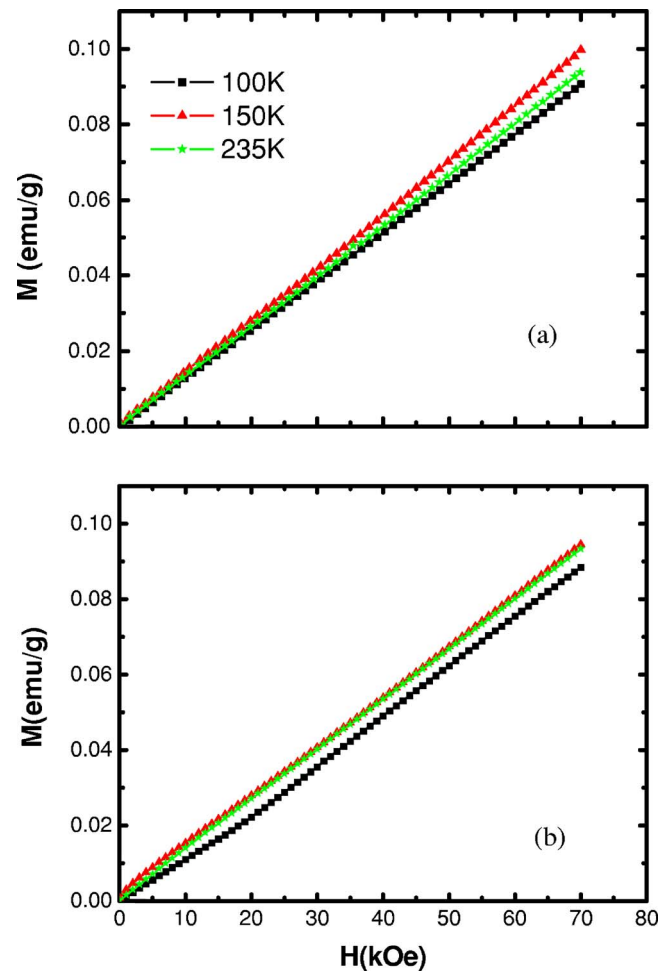


FIG. 4. (Color online) Magnetization curves at 100 K, 150 K, and 235 K for SA (a) and SO (b).

curves for these two samples at 100 K, 150 K, and 235 K are present in Figs. 4(a) and 4(b), respectively. In the temperature region of 175–280 K, no ferromagnetic component was detected from the linear magnetization curves. Therefore, the kink is attributed to a very short-range-ordering effect.¹³ The similar kink has also been found in $\text{La}_{0.6}\text{Sr}_{0.4}\text{FeO}_{3-y}$ and $\text{La}_{1/3}\text{Ca}_{2/3}\text{MnO}_3$.^{12,14} Moreover, a thermal hysteresis was observed between the field-cooled cooling (FCC) and field-cooled warming (FCW) process at 500 Oe, shown in the inset of Fig. 3(b), which may be the other proof for the existence of the short-range order. Such thermal hysteresis is not observed in SA, suggesting that the short-range order was blurred with increasing the oxygen vacancies. For the sample prepared in air, the increase in oxygen vacancies results in an increase in Fe^{3+} ions content. According to the Goodenough’s superexchange interaction theory,¹⁰ the superexchange interaction between $3d^5$ (Fe^{3+}) and $3d^5$ (Fe^{3+}) cations is antiferromagnetic, and is stronger than that between Fe^{4+} and Fe^{3+} ions, as well as that between Fe^{4+} and Fe^{4+} ions. Thus, the AFM order is strengthening promptly with increasing Fe^{3+} ions content, which results in a higher magnetic order temperature of SA.

The measurement of ac susceptibility ($\chi_{ac}=\chi'-i\chi''$) gives us a detailed insight into the dynamics of freezing. The tem-

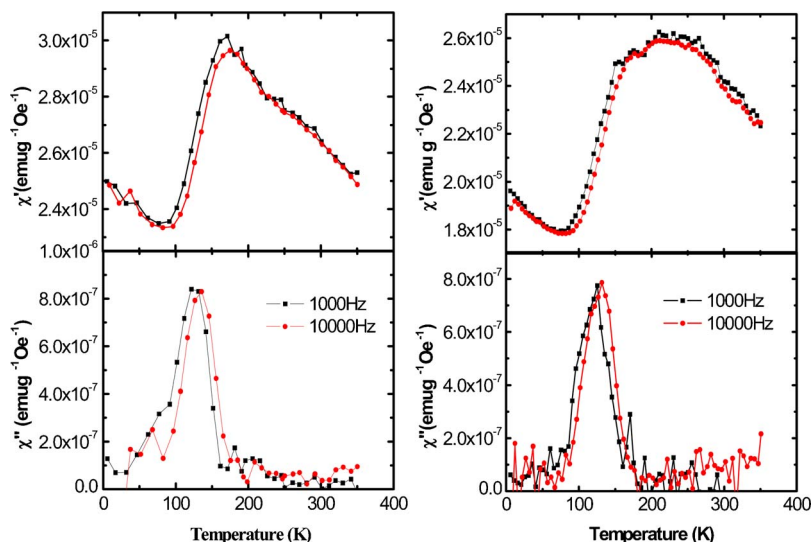


FIG. 5. (Color online) Temperature dependence of ac magnetic susceptibility under zero biasing fields for SA (a) and SO (b).

perature and frequency dependence of χ_{ac} measurements were made in the same run with changing frequency in a circular turn for these two samples without external field, shown in Figs. 5(a) and 5(b), respectively. The real component of susceptibility $\chi'(T)$ in these two samples display similar broad maxima at about 175 K, and that the position of the peak shifts to higher temperature (about 10 K) and the amplitude decreases slightly with increasing frequency. Since $\chi'(T)$ is proportional to the magnetic moment, the single peak is a credible indicator of magnetic phase transition. Similar χ' vs T behavior has been also observed in the disorder spinel system $Zn_xCo_{1-x}FeCrO_4$.¹⁵ The peak in $\chi'(T)$ is rather broad that may be the superposition of several peaks very close to each other, which means there exists many clusters with different sizes. The imaginary component of susceptibility $\chi''(T)$, which is related to the dissipated power, indicates broad peaks at $T \sim 130$ K with a shift to higher temperature with increasing frequency. These characters of $\chi'(T)$ and $\chi''(T)$ are related to spin-glass behavior but unlike the canonical spin-glass behavior,¹¹ which may be the sign of formation of some kind of clusters. The deformation point of $\chi''(T)$ indicates the onset of freezing, which corresponds to the point where $\chi'(T)$ starts to decrease with decreasing temperature because of increased difficulty in moving the magnetic moments and clusters. The peaks of $\chi''(T)$ are caused by the reversible remotion of cluster within one period of the ac.¹⁶ In an assembly of clusters formed out of short-range interactions, the freezing appears through the probability of each cluster to overcome the energy barrier E , which is expressed in terms of relaxation time $\tau = \tau_0 \exp(E/kT)$, where τ_0 is the preexponential factor and k is Boltzmann constant. An anomaly in $\chi'(T)$ will appear at T_f when τ becomes larger than the characteristic measuring time. On the other hand, if the relaxation time spectrum is very broad, this anomaly in ac susceptibility can be associated with the maximum or some average of the largest relaxation times of the distribution, thus $\chi'(T)$ in our experiment behaves as a very broad maxima. Furthermore, the characteristic time scale describing the spin dynamics τ_0 is estimated to be about 10^{-11} s for these two samples, which are slightly larger than the

typical values 10^{-12} s for canonical spin-glass systems.¹⁷ Such large characteristic time is related to the large sizes of the clusters. The freezing point T_f of 175 K derived from the ac susceptibility is consistent well with the result obtained from the temperature dependence of magnetization.

In order to elucidate the mechanism of cluster-glass-like behaviors of $La_{0.5}Ca_{0.5}FeO_{3-\delta}$, Mössbauer experiments at various temperatures were carried out to investigate the charge states of Fe ions in the cluster glass, AFM and paramagnetic states, shown in Figs. 6(a) and 6(b), respectively. For SO, the Mössbauer spectrum at RT exhibits a typical paramagnetic singlet with center shift (CS) of 0.20 ± 0.02 mm/s, which agrees well with the results reported in the literature.^{13,14} The singlet is corresponding to the average-valence charge state between Fe^{4+} and Fe^{3+} ions. The average-valence state may be caused by electron hopping between Fe^{4+} and Fe^{3+} ions, which are faster than the lifetime of the excited ^{57}Fe state. The observed relaxation broadening in the Mössbauer data is indicative of increasing short-range fluctuations in the spin structure. As for SA, in addition to a similar singlet with that of SO, two additional sextets with hyperfine fields of 364 kOe and 205 kOe, center shifts of 0.39 mm/s, and -0.20 mm/s, exist in the spectrum, which are assigned to be Fe^{3+} and Fe^{4+} ions, respectively. Consistent with magnetization measurements, Mössbauer spectra also indicate that T_N of SA is above RT and that of SO is below RT.

With lowering the temperature to 175 K, four magnetically split sextets coexists with one paramagnetic doublet for both samples. Among the four magnetically split sextets, one sextet with center shift of -0.1 mm/s is assigned to be Fe^{5+} ions. The ^{57}Fe hyperfine fields are 223 kOe for SA and 208 kOe for SO owing to the higher T_N of SA. Due to the appearance of Fe^{5+} ions, Fe^{3+} ions locate at two nonequivalent sites, i.e., without Fe^{5+} [$Fe(I)$] and with at least one Fe^{5+} [$Fe(II)$] as their neighborhood.⁷ Therefore, the subspectra corresponding to Fe^{3+} ions were fitted with the two sextets with the same center shift of 0.40 mm/s, whereas different hyperfine fields of 506 kOe and 456 kOe for SA as well as 474 kOe and 431 kOe for SO. The sextet with center shift of 0.1 mm/s and hyperfine fields of 254 kOe for SA and

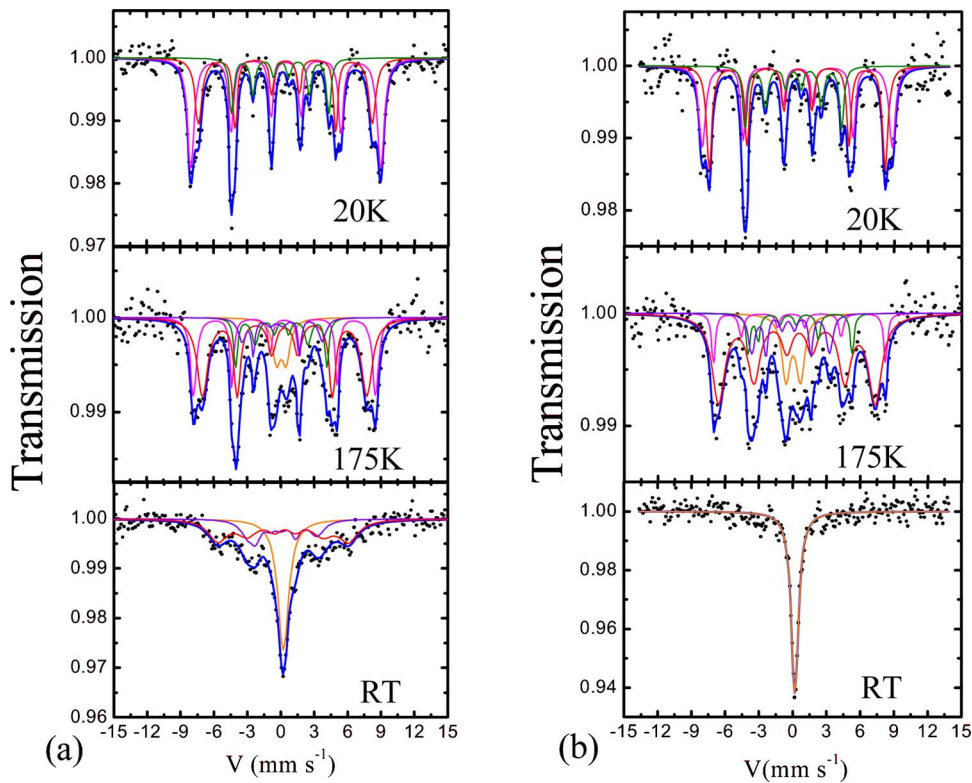


FIG. 6. (Color online) Mössbauer spectra of $\text{La}_{0.5}\text{Ca}_{0.5}\text{FeO}_{3-\delta}$ at various temperatures for SA (a) and SO (b).

284 kOe for SO is attributed from the Fe^{4+} ions. As illustrated in Figs. 7(a) and 7(b), it was observed that the content of Fe^{4+} ions was observed to decrease with decreasing temperature, and consequently the Fe^{5+} and Fe^{3+} ions contents increase with decreasing temperature. With further decreasing the temperature to 20 K, the best fitting to both samples can be reached by adopting three magnetic hyperfine fields,

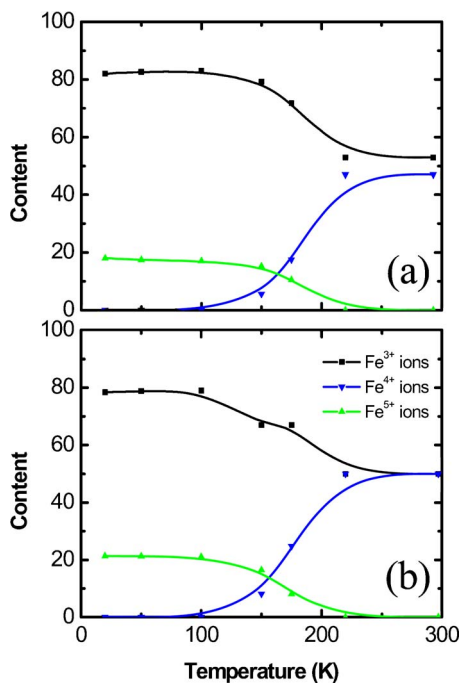


FIG. 7. (Color online) Temperature dependence of the concentration of Fe^{3+} , Fe^{4+} , and Fe^{5+} ions in SA (a) and SO (b).

corresponding to the three Fe ions sites, a Fe^{5+} site and two Fe^{3+} sites. No Fe^{4+} ions were detected in these two samples at 20 K. The detailed hyperfine parameters of these different Fe ions are summarized in Table II. Similar results were also obtained in $\text{La}_{1-x}\text{Sr}_x\text{FeO}_3$,¹⁸ Mössbauer spectra measured at various temperatures provide a clear evidence for the CD transition of Fe^{4+} ions into Fe^{3+} ions and Fe^{5+} ions.

On the basis of the relative absorption areas of the sub-spectra, the content of Fe^{5+} ions at 20 K is about 17% for SA and 22% for SO, respectively. Compared to the expectation of the $\text{Fe}^{4+}/\text{Ca}^{2+}$ ratio according to the charge balance, the actual ratio indicates that oxygen vacancies would compensate the charge balance in $\text{La}_{0.5}\text{Ca}_{0.5}\text{FeO}_{3-\delta}$. Therefore, we could obtain the relative number of oxygen vacancies in principle by the relative absorption area of Fe^{5+} ions on the basis of the electrostatic neutrality if cations have a random distribution of over available sites.¹⁹ The oxygen vacancy δ is roughly estimated to be 0.07 for SA and 0.03 for SO, respectively.

It was well known that the superexchange interactions between Fe^{3+} and Fe^{3+} ions, Fe^{4+} and Fe^{4+} as well as Fe^{3+} and Fe^{4+} ions in the Fe perovskites are antiferromagnetic. However, the CD transition of Fe^{4+} ions into Fe^{3+} ions and Fe^{5+} ions occurred at low temperature results in a ferromagnetic interaction between Fe^{3+} ($3d^5$) and Fe^{5+} ($3d^3$) along the 180° Fe—O—Fe pathway. The competition between ferromagnetic interaction and antiferromagnetic interaction induces the cluster-glass magnetic behaviors in $\text{La}_{0.5}\text{Ca}_{0.5}\text{FeO}_{3-\delta}$ perovskites. Since very weak ferromagnetic interaction between Fe^{3+} and Fe^{5+} ions compared with antiferromagnetic ones, these materials exhibit a significantly different glassy magnetic behavior as in the typical spin-glass system.

TABLE II. Hyperfine parameter of SA and SO deduced from Mössbauer spectra.

		SA			SO		
$T(K)$		20	175	RT	20	175	RT
Fe^{3+} (I)	$H_{hf}(kOe)$	527(3)	504(5)		524(5)	450(9)	
	CS(mm/s)	0.473(3)	0.4(1)		0.40(5)	0.4(0)	
	QS(mm/s)	-0.01(3)	-0.0(1)		-0.04(5)	0.4(2)	
	$W(mm/s)$	0.25(5)	0.3(1)		0.24(0)	0.4(2)	
	$R(\%)$	51(1)	28(1)		37(7)	23(2)	
Fe^{3+} (II)	$H_{hf}(kOe)$	481(4)	456(9)	364(20)	486(4)	439(7)	
	CS(mm/s)	0.42(4)	0.4(1)	0.3(3)	0.39(4)	0.3(1)	
	QS(mm/s)	0.01(4)	0.0(1)	-0.1(3)	-0.03(4)	-0.2(2)	
	$W(mm/s)$	0.25(8)	0.4(1)	0.7(3)	0.24(0)	0.5(2)	
	$R(\%)$	32(1)	40(1)	41(2)	41(7)	44(2)	
Fe^{5+}	$H_{hf}(kOe)$	270(4)	229(1)		267(5)	207(9)	
	CS(mm/s)	-0.01(6)	-0.1(1)		0.01(7)	-0.2(1)	
	QS(mm/s)	-0.04(6)	0.2(1)		-0.05(6)	0.2(1)	
	$W(mm/s)$	0.27(9)	0.3(3)		0.24(0)	0.3(1)	
	$R(\%)$	17(4)	12(1)		22(4)	15(6)	
Fe^{4+}	$H_{hf}(kOe)$		286(6)	205(2)		283(6)	
	CS(mm/s)		0.2(1)	-0.2(3)		0.2(1)	
	QS(mm/s)		0.1(3)	0.3(2)		0.5(1)	
	$W(mm/s)$		0.4(3)	0.6(4)		0.3(2)	
	$R(\%)$		11(0)	23(2)		8(5)	
$Fe^{3.5+}$	$H_{hf}(kOe)$		PM	PM		PM	PM
	CS(mm/s)		0.1(0)	0.2(1)		0.1(1)	0.2(0)
	QS(mm/s)		0.9(3)			1.2(2)	
	$W(mm/s)$		0.4(3)	0.6(1)		0.5(2)	0.4(0)
	$R(\%)$		9(3)	36(6)		12(6)	100

IV. CONCLUSION

On the basis of temperature dependence of dc magnetization in ZFC and FC curves, together with frequency dependence of ac susceptibility, a cluster-glass-like magnetic behavior was observed in $La_{0.5}Ca_{0.5}FeO_{3-\delta}$ with different oxygen vacancy contents. Mössbauer spectra measured at various temperatures indicated a CD transition from Fe^{4+} ions to Fe^{3+} and Fe^{5+} ions occurs at the freezing temperature of 175 K. The cluster-glass-like magnetic behavior origi-

nated from the competition of Fe^{3+} — Fe^{5+} ferromagnetic interaction and Fe^{3+} — Fe^{3+} antiferromagnetic interaction.

ACKNOWLEDGMENTS

This work was supported by the State Key Project of Fundamental Research, and the National Natural Sciences Foundation of China. One of the authors (Z. H. C.) thanks the Alexander von Humboldt Foundation for financial support and the generous donation of Mössbauer equipments.

*Corresponding author. Electronic address: zhcheng@aphy.iphy.ac.cn

¹J. Matsuno, T. Mizokawa, A. Fujimori, Y. Takeda, S. Kawasaki, and M. Takano, Phys. Rev. B **66**, 193103 (2002).

²S. J. Kim *et al.*, Phys. Rev. B **66**, 014427 (2002).

³R. Micnas, J. Ranninger, and S. Robaszkiewicz, Rev. Mod. Phys.

62, 113 (1990).

⁴S. Kawasaki, M. Takano, R. Kanno, T. Takeda, and A. Fujimori, J. Phys. Soc. Jpn. **67**, 1529 (1998).

⁵J. Q. Li, Y. Matsui, S. K. Park, and Y. Tokura, Phys. Rev. Lett. **79**, 297 (1997).

⁶J. B. Yang, X. D. Zhou, Z. Chu, W. M. Jikal, Q. Cai, J. C. Ho, D.

- C. Kundaliya, W. B. Yelon, W. J. James, H. U. Anderson, H. H. Hamdeh, and S. K. Malik, *J. Phys.: Condens. Matter* **15**, 5039 (2003).
- ⁷S. Komornicki, L. Fournes, J. C. Grenier, F. Menil, M. Pouchard, and P. Hagenmuller, *Mater. Res. Bull.* **16**, 967 (1981).
- ⁸J. Li, *Hyperfine Interact.* **69**, 573 (1991).
- ⁹P. M. Woodward, D. E. Cox, E. Moshopoulou, A. W. Sleight, and S. Morimoto, *Phys. Rev. B* **62**, 844 (2000).
- ¹⁰J. B. Goodenough, *Magnetism and Chemical Bond* (Wiley, New York, London, 1963).
- ¹¹S. Reich, Y. Tsabba, and G. Cao, *J. Magn. Magn. Mater.* **202**, 119 (1999).
- ¹²J. B. Yang, W. B. Yelon, W. J. James, Z. Chu, M. Kornecki, Y. X. Xie, X. D. Zhou, H. U. Anderson, Amish G. Joshi, and S. K. Malik, *Phys. Rev. B* **66**, 184415 (2002).
- ¹³M. Takano and Y. Takeda, *Bull. Inst. Chem. Res., Kyoto Univ.* **61**, 406 (1983).
- ¹⁴H. D. Zhou, G. Li, S. J. Feng, Y. Liu, T. Qian, X. J. Fan and X. G. Li, *Solid State Commun.* **122**, 507 (2002).
- ¹⁵R. Chakravarthy, L. Madhav Rao, S. K. Paranjpe, S. K. Kulushrestha, and S. B. Roy, *Phys. Rev. B* **43**, 6031 (1991).
- ¹⁶S. Pechev, B. Chevalier, D. Laffague, B. Darriet, T. Roisnel, and J. Etourneau, *J. Magn. Magn. Mater.* **191**, 282 (1999).
- ¹⁷J. A. Mydosh, *Spin Glass: An Experimental Introduction* (Taylor and Francis, London, Washington, DC, 1993).
- ¹⁸S. E. Dann, D. B. Currie, M. T. Weller, M. F. Thomas, and A. D. Al-Rawwas, *J. Solid State Chem.* **109**, 134 (1994).
- ¹⁹E. Mashkina, C. McCammon, and F. Seifert, *J. Solid State Chem.* **177**, 262 (2004).